

Accurate Mapping of RNNs on Neuromorphic Hardware with Adaptive Spiking Neurons

Gauthier Boeshertz
gauthier.boeshertz@gmail.com
ETH Zurich, Switzerland

Manu Nair*
manu@synthara.ai
Synthara, Switzerland

Giacomo Indiveri
giacomo@ini.uzh.ch
Institute of Neuroinformatics, University of Zurich and
ETH Zurich, Switzerland

Alpha Renner*
a.renner@fz-juelich.de
Forschungszentrum Jülich, Germany

ABSTRACT

Thanks to their parallel and sparse activity features, recurrent neural networks (RNNs) are well-suited for hardware implementation in low-power neuromorphic hardware. However, mapping rate-based RNNs to hardware-compatible spiking neural networks (SNNs) remains challenging. Here, we present a $\Sigma\Delta$ -low-pass RNN (lpRNN): an RNN architecture employing an adaptive spiking neuron model that encodes signals using $\Sigma\Delta$ -modulation and enables precise mapping. The $\Sigma\Delta$ -neuron communicates analog values using spike timing, and the dynamics of the lpRNN are set to match typical timescales for processing natural signals, such as speech. Our approach integrates rate and temporal coding, offering a robust solution for the efficient and accurate conversion of RNNs to SNNs. We demonstrate the implementation of the lpRNN on Intel’s neuromorphic research chip Loihi, achieving state-of-the-art classification results on audio benchmarks using 3-bit weights. These results call for a deeper investigation of recurrency and adaptation in event-based systems, which may lead to insights for edge computing applications where power-efficient real-time inference is required.

KEYWORDS

Neuromorphic computing, Neuromorphic engineering, Sigma-delta neuron, Edge Computing, Audio classification, Recurrent neural networks (RNNs), Spiking neural networks (SNNs), Intel Loihi

1 INTRODUCTION

Neuromorphic computing [18] aims to build computing systems using principles derived from neural systems of animal brains. Its common design features, geared toward improved efficiency compared to conventional architectures, are massive parallelism, near- or in-memory computation, and asynchronous communication using unary events (spikes). Recurrently connected networks (RNN) that have a state that evolves over time make the best use of these principles [8]. After being initially sidelined by the Transformer’s [32]

* equal contribution

This paper was accepted at the IEEE/ACM International Conference on Neuromorphic Systems, July 30–Aug 2, 2024, Arlington, VA

©2024 IEEE. Personal use of this material is permitted. Permission from IEEE must be obtained for all other uses, in any current or future media, including reprinting/republishing this material for advertising or promotional purposes, creating new collective works, for resale or redistribution to servers or lists, or reuse of any copyrighted component of this work in other works.

strong performance in natural language processing (NLP) [5], RNNs are now experiencing a revival [16, 23] due to their linear scaling with the number of inputs.

Despite methods like surrogate gradients [2, 21] and training frameworks [13] overcoming initial issues, translating Artificial Neural Network (ANN) progress to Spiking Neural Networks (SNNs) and neuromorphic hardware remains challenging [25]. Two main approaches exist:

- 1) Directly training SNNs inherently accounts for constraints like quantization and enables efficient spike timing codes [21, 29, 37].
- 2) ANN-SNN conversion converts trained ANNs to SNNs [13], which allows leveraging the most recent advances in ANNs, such as regularizers or network structures.

While conversion works well for feedforward convolutional networks in computer vision [12], for RNNs, where small deviations accumulate, conversion approaches are rare [11].

In this work, we extend and validate an RNN conversion approach [19] on Intel’s digital neuromorphic research chip Loihi [7]. The approach solves the RNN conversion issue in two ways: First, the sigma-delta ($\Sigma\Delta$) spiking neuron model [19, 20, 24, 35, 36], analogous to adaptive linear integrate-and-fire (aLIF) models [3, 4, 20], provides a precise way to map analog activations to spikes, allowing an approximation with a controlled error. The $\Sigma\Delta$ -neuron combines aspects of rate and temporal coding, representing signals through spike timings rather than just firing rates. Second, we integrate the $\Sigma\Delta$ -neurons into a low-pass recurrent neural network (lpRNN) architecture. The lpRNN’s slower dynamics make RNN to SNN mapping easier and cheaper, matching typical timescales in speech and biomedical applications. Finally, we test the model in non-spiking and spiking simulation and on Intel’s neuromorphic research chip Loihi on two benchmark datasets and set a new state-of-the-art for on-chip speech classification.

2 MODEL

2.1 The $\Sigma\Delta$ -spiking neuron model

In this work, we adapt the aLIF/ $\Sigma\Delta$ -neuron [3, 19, 24, 35, 36] and implement it on the Loihi [7] neuromorphic chip. Due to its four state variables, the model requires two compartments on Loihi 1. $\Sigma\Delta$ -neurons communicate analog signals by transmitting spikes only when the difference between an internal state and the input exceeds a threshold. It can be described on Loihi with the following

discrete-time dynamics equations, adapted from the aLIF [19]:

$$I_{mem}(t+1) = I_{mem}(t) - \frac{I_{mem}(t)}{\tau_{mem}} + i - s \quad (1)$$

$$s(t+1) = s(t) - \frac{s(t)}{\tau_s} + w_{fb}\delta_i \quad (2)$$

$$i(t+1) = i(t) - \frac{i(t)}{\tau_i} + u(t) \quad (3)$$

$$u(t+1) = u(t) - \frac{u(t)}{\tau_u} + \sum_{n=1}^N \delta_n W_n^{SNN} \quad (4)$$

Where I_{mem} represents the neuron’s membrane potential, s is the adaptation/feedback current, i is the input current, b^{SNN} is the bias, u is the weighted (by W_n^{SNN}) and filtered input from presynaptic spike trains (δ_n) or from an analog input signal (not shown), and τ_{mem} , τ_s , τ_i , τ_u are time constants. The neuron spikes when I_{mem} exceeds a threshold, at which point I_{mem} is reset to 0. This spike is transmitted to postsynaptic neurons and recursively added as a feedback spike train δ_i weighted by w_{fb} to s . This mechanism allows s to track i and serve as the neuron’s internal activation state corresponding to an ANN activation value. Intuitively, whenever s diverges from i too much, a spike is produced to correct it (see Fig. 1b). This activation state can either be read out directly from s or reconstructed by the output spikes. The model as a block diagram is shown in Fig. 1a.

2.2 The low-pass RNN model

The $\Sigma\Delta$ -neuron model’s feedback current s corresponds to an ANN activation value y , enabling the mapping of RNNs to SNNs. Moreover, the additional filtering of the input current i implements a low-pass behavior, leading to a longer memory and, therefore, better performance than vanilla RNNs on specific tasks. Therefore, we term this the low-pass RNN (lpRNN), with non-spiking dynamics described by:

$$y_t = \alpha \odot y_{t-1} + (1 - \alpha) \odot \sigma(W_{rec} \cdot y_{t-1} + W_{in} \cdot x_t + b) \quad (5)$$

where σ is a non-linearity, \odot the element-wise (Hadamard) product, and \cdot matrix multiplication. x_t the input vector, y_t the output vector, the subscripts indicate the time step, W_{rec} and W_{in} the recurrent and input weight matrices, and b the biases. Here, α , a (reciprocal) time constant, is a fixed hyperparameter optimized by hyperparameter search but could be trained individually. α can be mapped to the time constants of the Spiking Neural Network (SNN) by $\tau = \frac{-T_s}{\log \alpha}$ where T_s is the duration of the ANN algorithmic timestep or sampling interval of the input data-stream fed to the recurrent ANN. The nonlinearity σ is a clamped ReLU as spiking neurons naturally implement a ReLU by not allowing a negative s [3, 35]. It is clamped to I_{in} because the Low-Pass Filter (LPF) property of the $\Sigma\Delta$ -neuron limits the maximum activity to I_{in} .

While the ANN time resolution is given by the data sampling rate, the SNN requires a finer time resolution because the timing and the number of spikes matter. Therefore, the time constants are scaled by the ratio of the ANN and SNN algorithmic time steps, $\tau_{SNN} = \frac{T_{ANN}}{T_{SNN}} \tau_{ANN}$. Due to constraints in the maximal neural state values on the Loihi chip, we use only 3 of the available 8-bit weight precision. Consequently, we train the ANN using 3-bit quantized

Table 1: Top-1 Accuracy comparison on HD and SHD (20 classes).

Method		Weight precision (bits)	Acc. (%)
SHD	SNN RadLIF [2]	32	94.6
	Learned Delays [17]	32	95.1
	ANN liBRU [2]	32	99.96
HD	GRU [2]	32	99.91
	lpRNN [this work]	3	99.69
	SNN RLIF [2]	32	99.35
	lpRNN [this work]	3	99.69
	Loihi Speech2Spikes [30]	7	97.5
	lpRNN [this work]	3	99.33

weights in a quantization-aware manner via a straight-through estimator (STE) [1].

The architecture used in this work, shown in Fig. 2, consists of a feedforward low-pass layer to encode input signals into spikes, followed by two recurrent low-pass layers and an output layer. This compact size was chosen to avoid overfitting on the given datasets.

3 RESULTS

We evaluate on two audio benchmark datasets commonly used for ANNs and SNNs: The Heidelberg Digits (HD) [6] and Google Speech Commands (GSC) [33]. For both datasets, we follow the same preprocessing, training, and testing procedure. The audio is transformed into Mel spectrograms, a common non-linear transformation [10, 17, 34] emphasizing lower frequencies where useful sounds reside [9]. We train the ANN weights and then transfer the network to an SNN for inference on the unseen test set. The input data is encoded into spikes using Brian2 [31], simulating the input to the low-pass feedforward layer. The recurrent and output layers are run on Loihi and, as a baseline, in a Brian2 simulation. Further details are provided in the Methods and code (to be released).

The Heidelberg Digits (HD) [6] contains 10,000 recordings of 20 classes of digits in English and German. Instead of using the provided Spiking (SHD) version with spikes from an artificial cochlear model, we encode the raw audio Mel spectrograms using the $\Sigma\Delta$ -neuron model. This approach produces fewer spikes (around 5600 vs. 8230 per test sample) while achieving better accuracy. As shown in Table 1, the lpRNN outperforms the only previous neuromorphic approach [30] and matches state-of-the-art ANN and SNN methods. However, the near-perfect results indicate this dataset may not ideally differentiate model performance.

The Google Speech Commands (GSC) [33] contains one-second audio recordings of spoken words to be classified. We evaluate three variants: GSCv1 with 36 words and GSCv2 with 12 or 36 classes. To improve ANN-SNN mapping, we apply pruning [14] to reduce mismatch from low-activity neurons when $I_{in} \gg activity$. Table 2 compares results. The lower performance on GSCv2-36, compared to the best SNNs, is potentially due to using only 3-bit weights without batch normalization. The lpRNN again outperforms the previous neuromorphic approaches.

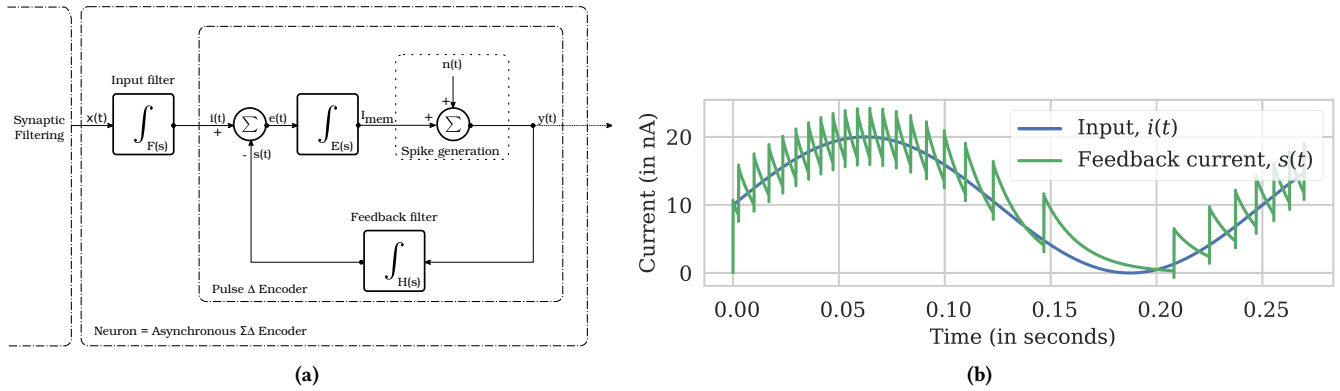


Figure 1: a. Block diagram of a $\Sigma\Delta$ -neuron. b. Evolution of the feedback signal $s(t)$ following the the input. Whenever it decays too far below the input, the neuron generates a spike ($y(t)$) which increases the feedback current. Panels from [19].

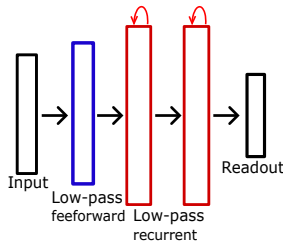


Figure 2: Architecture of the lpRNN network.

Table 2: Top-1 accuracy comparison on the variants of the Google Speech Commands dataset

	Weight precision (bits)	v1-36w	v2-12w	v2-35w
Non-spiking				
Att RNN [10]	32	94.3	96.9	93.9
AS Transformer [15]	32			98.1
lpRNN ANN [this work]	3	93.56	95.07	94.03
Spiking				
SRNN [34]	32		92.1	
LSNN [28]	32		91.2	
SLAYER [22]	32		91.74	
RLIF [2]	32			93.58
RadLIF [2]	32			94.51
Learned Delays [17]	32			95.29
lpRNN SNN [this work]	3	93.19	93.13	93.33
Neuromorphic Hardware				
Speech2Spikes [30]	7			71.1
Spinnaker2 Eprop [26]	32		91.12	
lpRNN Loihi [this work]	3	92.08	92.8	92.4

4 DISCUSSION

The lpRNN using $\Sigma\Delta$ -neurons allows faithful conversion from Recurrent Neural Network (RNN) to SNN. We present one of the

first results on a neuromorphic chip achieving comparable performance to RNN and SNN implemented on standard computing architectures. We demonstrate state-of-the-art results in the HD dataset in the SNN setting and strong results on GSC. This is achieved by training the network using backpropagation through time (BPTT) with the standard pipeline for ANNs and then transferring it to neuromorphic hardware with constraints on the quantization of weights (3-bit) and timesteps.

These results provide additional evidence that synaptic dynamics and neuronal adaptation are important mechanisms for encoding natural data with the $\Sigma\Delta$ -mechanism. Most SNN methods in Table 2 use adaptive neuron models [2, 28, 34], generally outperforming non-adaptive models. Adaptation mechanisms that change the neuron spiking threshold, instead of subtracting an adaptation variable $s(t)$ from the membrane potential (Eq.2), are equivalent; they both change the amount of input needed until the threshold is reached.

Compared to ANN models, the lpRNN achieves results comparable to the commonly used gated RNNs (GRU and LSTM) on both datasets. This suggests that complex models with many parameters are not needed for time series without fast changes and without long-term dependencies, such as audio and biomedical data. However, for much longer sequences like sentences or documents, gated RNNs, state-space models, or transformers may be more suitable. Therefore, here, we focus on simple keyword spotting tasks, but the results encourage further exploration of the $\Sigma\Delta$ -model, independently of the network architecture. The $\Sigma\Delta$ -model is of particular interest for robust encoding and computation in ultra-low power analog hardware [20, 27]. Training the synaptic delays (as [17]) and time constants α individually might broaden the range of time scales of the network dynamics, making it suitable for additional applications.

5 METHODS

The ANN simulations were made using Pytorch 1.9 and the SNN simulations with Brian2 [31]. Loihi experiments were conducted remotely using NxSDK version 0.9.9 on the Nahuku32 board ncl-ghrd-01.

On Loihi, neurons can be created from one or more compartments. A compartment’s input current can integrate spikes, and

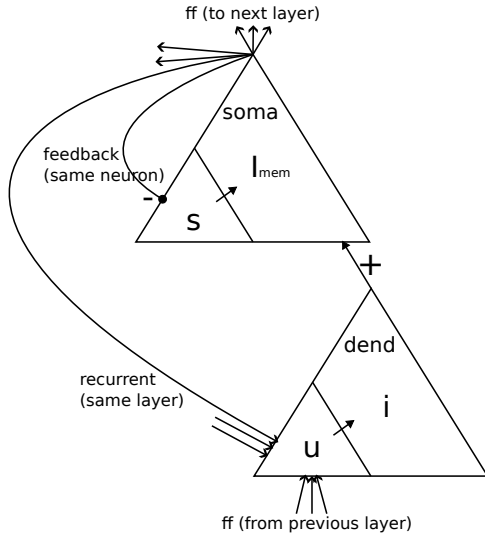


Figure 3: Multi-compartment $\Sigma\Delta$ -neuron on Loihi

then this current is further integrated into the membrane potential. These signals can be relayed between compartments via connecting dendrites. The low-pass neuron comprises two compartments, as shown in Fig 3. The ‘dendritic’ compartment integrates the spikes coming from recurrent and feedforward connections into the input current u . The ‘membrane potential’ i of this compartment is then added to the membrane potential I_{mem} of the ‘somatic’ compartment. This second compartment is connected to itself with an inhibitory synapse such that the spikes it generates are integrated into the adaptation/feedback current s .

The weights and biases for Loihi are obtained from the ANN as follows:

$$W^{SNN} = \frac{fW^{ANN}}{\tau_u * \tau_i * 64} \quad b^{SNN} = \frac{fb^{ANN}}{\tau_i} \quad (6)$$

A factor f is used to scale the weights to make the best use of the precision available on the chip. Because the value of the state variables is bounded by $\pm 2^{23}$ (24 bits), f cannot be chosen too large to avoid overflow. A lower f , however, leads to lower weight precision, as weights are constrained to integer values.

ACKNOWLEDGMENTS

The authors thank Intel Labs for providing access to the Loihi research hardware. A.R. discloses support from the University of Zurich postdoc grant [FK-21-136] and the VolkswagenStiftung [CLAM 9C854].

REFERENCES

- [1] Yoshua Bengio, Nicholas Léonard, and Aaron Courville. 2013. Estimating or propagating gradients through stochastic neurons for conditional computation. *arXiv preprint arXiv:1308.3432* (2013).
- [2] Alexandre Bittar and Philip N Garner. 2022. A surrogate gradient spiking baseline for speech command recognition. *Frontiers in Neuroscience* 16 (2022), 865897. <https://doi.org/10.3389/fnins.2022.865897>
- [3] Sander M Bohte. 2012. Efficient spike-coding with multiplicative adaptation in a spike response model. In *Advances in Neural Information Processing Systems*.

- [4] Romain Brette and Wulfram Gerstner. 2005. Adaptive exponential integrate-and-fire model as an effective description of neuronal activity. *Journal of Neurophysiology* 94, 5 (2005), 3637–3642. <https://doi.org/10.1152/jn.00686.2005>
- [5] Tom Brown, Benjamin Mann, Nick Ryder, Melanie Subbiah, Jared D Kaplan, Prafulla Dhariwal, Arvind Neelakantan, Pranav Shyam, Girish Sastry, Amanda Askell, et al. 2020. Language models are few-shot learners. In *Advances in Neural Information Processing Systems*, Vol. 33. 1877–1901.
- [6] Benjamin Cramer, Yannik Stradmann, Johannes Schemmel, and Friedemann Zenke. 2020. The Heidelberg spiking data sets for the systematic evaluation of spiking neural networks. *IEEE Transactions on Neural Networks and Learning Systems* 33, 7 (2020), 2744–2757. <https://doi.org/10.1109/TNNLS.2020.3044364>
- [7] Mike Davies, Narayan Srinivasa, Tsung-Han Lin, Gautham Chinya, Yongqiang Cao, Sri Harsha Choday, Georgios Dimou, Prasad Joshi, Nabil Imam, Shweta Jain, et al. 2018. Loihi: A neuromorphic manycore processor with on-chip learning. *IEEE Micro* 38, 1 (2018), 82–99. <https://doi.org/10.1109/MM.2018.112130359>
- [8] Mike Davies, Andreas Wild, Garrick Orchard, Yulia Sandamirskaya, Gabriel A Fonseca Guerra, Prasad Joshi, Philipp Plank, and Sumedh R Risbud. 2021. Advancing neuromorphic computing with Loihi: A survey of results and outlook. *Proc. IEEE* (2021). <https://doi.org/10.1109/JPROC.2021.3067593>
- [9] Steven Davis and Paul Mermelstein. 1980. Comparison of parametric representations for monosyllabic word recognition in continuously spoken sentences. *IEEE Transactions on Acoustics, Speech, and Signal Processing* 28, 4 (1980), 357–366. <https://doi.org/10.1109/TASSP.1980.1163420>
- [10] Douglas Coimbra de Andrade, Sabato Leo, Martin Loesener Da Silva Viana, and Christoph Bernkopf. 2018. A neural attention model for speech command recognition. *arXiv preprint arXiv:1808.08929* (2018).
- [11] Peter U Diehl, Guido Zarella, Andrew Cassidy, Bruno U Pedroni, and Emre Neftci. 2016. Conversion of artificial recurrent neural networks to spiking neural networks for low-power neuromorphic hardware. In *2016 IEEE International Conference on Rebooting Computing (ICRC)*. IEEE, 1–8. <https://doi.org/10.1109/ICRC.2016.7738691>
- [12] Jianhao Ding, Zhaofei Yu, Yonghong Tian, and Tiejun Huang. 2021. Optimal ANN-SNN conversion for fast and accurate inference in deep spiking neural networks. *arXiv preprint arXiv:2105.11654* (2021).
- [13] Jason K Eshraghian, Max Ward, Emre O Neftci, Xinxin Wang, Gregor Lenz, Girish Dwivedi, Mohammed Bannamoun, Doo Seok Jeong, and Wei D Lu. 2023. Training spiking neural networks using lessons from deep learning. *Proc. IEEE* (2023). <https://doi.org/10.1109/JPROC.2023.3308088>
- [14] Jonathan Frankle and Michael Carbin. 2019. The lottery ticket hypothesis: Finding sparse, trainable neural networks. *arXiv preprint arXiv:1803.03635* (2019).
- [15] Yuan Gong, Yu-An Chung, and James Glass. 2021. Ast: Audio spectrogram transformer. *arXiv preprint arXiv:2104.01778* (2021).
- [16] Albert Gu and Tri Dao. 2023. Mamba: Linear-time sequence modeling with selective state spaces. *arXiv preprint arXiv:2312.00752* (2023).
- [17] Ilyass Hammouamri, Ismail Khalfouli-Hassani, and Timothée Masquelier. 2023. Learning Delays in Spiking Neural Networks using Dilated Convolutions with Learnable Spacings. *arXiv preprint arXiv:2306.17670* (2023).
- [18] Carver Mead. 1990. Neuromorphic electronic systems. *Proc. IEEE* 78, 10 (1990), 1629–1636. <https://doi.org/10.1109/5.58356>
- [19] Manu V Nair and Giacomo Indiveri. 2019. Mapping high-performance RNNs to in-memory neuromorphic chips. *arXiv preprint arXiv:1905.10692* (2019).
- [20] Manu V Nair and Giacomo Indiveri. 2019. An Ultra-Low Power Sigma-Delta Neuron Circuit. In *2019 IEEE International Symposium on Circuits and Systems (ISCAS)*. IEEE, 1–5. <https://doi.org/10.1109/ISCAS.2019.8702500>
- [21] Emre O Neftci, Hesham Mostafa, and Friedemann Zenke. 2019. Surrogate gradient learning in spiking neural networks. *IEEE Signal Processing Magazine* 36, 6 (2019), 61–63. <https://doi.org/10.1109/MSP.2019.2931595>
- [22] Garrick Orchard, E Paxon Frady, Daniel Ben Dayan Rubin, Sophia Sanborn, Sumit Bam Shrestha, Friedrich T Sommer, and Mike Davies. 2021. Efficient Neuromorphic Signal Processing with Loihi 2. In *2021 IEEE Workshop on Signal Processing Systems (SiPS)*. IEEE, 254–259. <https://doi.org/10.1109/SiPS52927.2021.00053>
- [23] Antonio Orvieto, Samuel L Smith, Albert Gu, Anushan Fernando, Caglar Gulcehre, Razvan Pascanu, and Soham De. 2023. Resurrecting recurrent neural networks for long sequences. In *International Conference on Machine Learning*. PMLR.
- [24] Peter O’Connor, Efstratios Gavves, and Max Welling. 2017. Temporally efficient deep learning with spikes. *arXiv preprint arXiv:1706.04159* (2017).
- [25] Alpha Renner, Forrest Sheldon, Anatoly Zlotnik, Louis Tao, and Andrew Sornborger. 2021. The Backpropagation Algorithm Implemented on Spiking Neuromorphic Hardware. *arXiv preprint arXiv:2106.07030* (2021). <https://arxiv.org/abs/2106.07030>
- [26] Amirhossein Rostami, Bernhard Vogginger, Yexin Yan, and Christian G Mayr. 2022. E-prop on SpiNNaker 2: Exploring online learning in spiking RNNs on neuromorphic hardware. *Frontiers in Neuroscience* 16 (2022), 1018006. <https://doi.org/10.3389/fnins.2022.1018006>

- [27] Arianna Rubino, Can Livanelioglu, Ning Qiao, Melika Payvand, and Giacomo Indiveri. 2020. Ultra-Low-Power FDSOI Neural Circuits for Extreme-Edge Neuromorphic Intelligence. *IEEE Transactions on Circuits and Systems I: Regular Papers* 68, 1 (2020), 45–56. <https://doi.org/10.1109/TCSI.2020.3035575>
- [28] Darjan Salaj, Anand Subramoney, Ceca Krašniković, Guillaume Bellec, Robert Legenstein, and Wolfgang Maass. 2021. Spike frequency adaptation supports network computations on temporally dispersed information. *Elife* 10 (2021), e65459. <https://doi.org/10.7554/eLife.65459>
- [29] Sumit Bam Shrestha and Garrick Orchard. 2018. Slayer: Spike layer error reassignment in time. In *Advances in Neural Information Processing Systems*. 1412–1421.
- [30] Kenneth M Stewart, Timothy Shea, Noah Pacik-Nelson, Eric Gallo, and Andreea Danielescu. 2023. Speech2spikes: Efficient audio encoding pipeline for real-time neuromorphic systems. In *Proceedings of the 2023 Annual Neuro-Inspired Computational Elements Conference*. 71–78. <https://doi.org/10.1145/3584954.3584995>
- [31] Marcel Stimberg, Romain Brette, and Dan FM Goodman. 2019. Brian 2, an intuitive and efficient neural simulator. *Elife* 8 (2019), e47314. <https://doi.org/10.7554/eLife.47314>
- [32] Ashish Vaswani, Noam Shazeer, Niki Parmar, Jakob Uszkoreit, Llion Jones, Aidan N Gomez, Lukasz Kaiser, and Illia Polosukhin. 2017. Attention is all you need. In *Advances in Neural Information Processing Systems*, Vol. 30.
- [33] Pete Warden. 2018. Speech commands: A dataset for limited-vocabulary speech recognition. *arXiv preprint arXiv:1804.03209* (2018).
- [34] Bojian Yin, Federico Corradi, and Sander M Bohte. 2021. Accurate and efficient time-domain classification with adaptive spiking recurrent neural networks. *arXiv preprint arXiv:2103.12593* (2021).
- [35] Young C Yoon. 2016. Lif and simplified SRM neurons encode signals into spikes via a form of asynchronous pulse sigma–delta modulation. *IEEE transactions on neural networks and learning systems* 28, 5 (2016), 1192–1205. <https://doi.org/10.1109/TNNLS.2016.2526029>
- [36] Davide Zambrano and Sander M Bohte. 2016. Fast and efficient asynchronous neural computation with adapting spiking neural networks. *arXiv preprint arXiv:1609.02053* (2016).
- [37] Friedemann Zenke and Surya Ganguli. 2018. Superspike: Supervised learning in multilayer spiking neural networks. *Neural computation* 30, 6 (2018), 1514–1541. https://doi.org/10.1162/neco_a_01086